Talanta 178 (2018) 563–568

Contents lists available at ScienceDirect

Talanta

journal homepage: www.elsevier.com/locate/talanta

Stimulus-response click chemistry based aptamer-functionalized mesoporous silica nanoparticles for fluorescence detection of thrombin

Zhonghui Chen, Mi Sun, Fang Luo, Kefeng Xu, Zhenyu Lin, Lan Zhang*

Ministry of Education Key Laboratory for Analytical Science of Food Safety and Biology, Fujian Provincial Key Laboratory of Analysis and Detection for Food Safety, Department of Chemistry, Fuzhou University, Fuzhou, Fujian 350116, China

ARTICLE INFO

Keywords:
Click chemistry
Mesoporous silica nanoparticles
Controlled release system
Aptamer
Fluorescence

ABSTRACT

In most aptamer based stimulus response mesoporous silica nanoparticles (MSN) systems, the aptamer is modified on the MSN via electrostatic interaction, however leakage might exist after a certain time in the system and hence the stability is not good. In this study, the pores of MSN were capped by aptamer through click chemistry reaction for the first time and the system was then employed to develop a fluorescence biosensor. Specifically, the aptamer of the target (thrombin in this study) was hybridized with its complementary DNA (which was initially modified with alkyne at the terminal) to form a double strand DNA (dsDNA) firstly, and then this dsDNA was modified on N_3 modified MSN via Cu(I) catalyzed alkyne-azide cycloaddition reaction. The guest molecules (fluorescein) were blocked in the pores of the MSN with high efficiency and nearly no leakage was detected. Upon the introduction of thrombin, thrombin specifically recognized its aptamer, so aptamer released from the MSN; and the single strand DNA(ssDNA) left could not cap the pores of the MSN efficiently and hence caused the releasing of fluorescein into the solution. The enhanced fluorescence intensity of the system has a good linear relationship with the thrombin concentration in the range of 50–1000 ng mL^{-1} with a detection limit of 28.46 ng mL^{-1}. The proposed biosensor has been successfully applied to detect thrombin in serum samples with high selectivity. The same strategy can be applied to develop biosensors for different targets by changing the adopted aptamer.

1. Introduction

Mesoporous silica nanoparticle (MSN) has sparked increasing interest in biomedical applications owing to the gradually increased requirements from clinical patients for high-performance therapeutic nanoformulations [1]. Many studies have focused on the application of MSN in controlled release system [2–6]. Such system normally adopts nanoparticles, polymers, small organic molecules, supramolecular assemblies, and biomolecules as capping agents to control the pores of MSN [7–11]. The release of guest molecules can be triggered by physical or chemical stimuli, such as pH, temperature, light, antibodies, enzymes, and nucleotides [12–17].

Aptamers are single-stranded DNA or RNA oligonucleotides that can specifically recognize their targets with high affinity and specificity. Many investigations have designed stimulus response controlled release system using aptamer as capping agent. For example, polyvalent MSN/aptamer bioconjugates were fabricated to target breast cancer cells (MCF-7) [18]. Zhu et al. reported a stimulus response fluorescence biosensor for adenosine triphosphate (ATP) [7]. MSN support was firstly loaded with fluorescein, aptamer-modified Au nanoparticles were used to cap the pores of MSN; upon the addition of ATP, the high affinity and specificity between ATP and its aptamer eventually caused the release of fluorescein from the capped pores. Tang et al. presented a novel target-aptamer-responsive controlled release system for ATP detection [19]; when glucose was loaded in the MSN pore, a commercially personal glucose meter was used to detect ATP based on the glucose released form the MSN. Zhang et al. designed a sensitive method for Hg^{2+} detection using DNA-capped MSN [20]. Two single-stranded DNA were cross-link on the MSN surface, they hybridized with T-base-rich linker DNA to cap dye in the MSN pore; in the presence of Hg^{2+}, T-Hg-T was formed, causing the releasing of dye from MSN. Our group reported a chemiluminescence biosensor for cocaine determination based on the stimulus response system [21]; glucose was initially loaded into MSN support, the interaction between positively charged MSN and negatively charged aptamer led to the capping of pores; the release of glucose was triggered via the introduction of cocaine. However, in most of reported stimulus response aptamer functionalized MSN system, the aptamer was modified on the surface of MSN to block the pores via

* Corresponding author.
E-mail address: zlan@fzu.edu.cn (L. Zhang).

http://dx.doi.org/10.1016/j.talanta.2017.09.043
Received 22 June 2017; Received in revised form 13 September 2017; Accepted 16 September 2017
Available online 19 September 2017

electrostatic interaction (specifically, negatively aptamer interacted with positively charged MSN to cap the pore, however, the pH of buffer in controlled release system notably affected aptamer binding to MSN), the leakage might exist after a long time so the stability was not high enough. It is necessary to build some simple capping way with higher stability and efficiency.

Since the first report of click chemistry in 2001 [22], the past years have witnessed an exponential increase in study regarding click chemistry [23–25]. One of the most studied reactions is Cu(I) catalyzed alkyne-azide cycloaddition reaction (CuAAC), it is simple and normally performed in mild conditions like H_2O solvent, even in the presence of many other functional groups with high efficiency [26]. CuAAC reaction has been successfully employed in the process of functionalization and modification (such as protein, cell, nanoparticle, etc.) [27–29]. To the best of our knowledge, no study has been reported on capping pores of MSN via chick chemistry reaction in the controlled release system.

In this study, the pores of MSN were capped by double stranded DNA (dsDNA) through CuAAC to develop a controlled release system for the first time. More specifically, N_3 was modified on the surface of MSN firstly to form N_3-MSN, then an alkyne modified dsDNA containing thrombin aptamer was modified on N_3-MSN through CuAAC to cap the pores of MSN with high efficiency. The target (thrombin in this study) combined with its aptamer with high affinity [30] and hence caused the releasing of aptamer from the MSN. As ssDNA could not block the pores of MSN with high efficiency, the fluorescein (which was initially blocked in the pores of the MSN) was released into the solution system and the fluorescence of the system increased. The proposed stimulus response system was then applied to detect thrombin in the serum samples with satisfied results.

2. Experimental sections

2.1. Reagents

Thrombin was purchased from Sigma-Aldrich Chemical Co (USA); Copper iodide (CuI), tris[(1-benzyl-1H-1,2,3-triazol-4-yl)methyl] amine (TBTA), and fluorescein isothiocyanate (FITC) were purchased from J & K Scientific Ltd. (Beijing, China). Trimethyl chlorosilane (TMCS), sodium hydroxide solution (NaOH), cetyltrimethyl ammonium bromide (CTAB), tetraeth-oxysilane (TEOS), and ethanol were purchased from Shanghai Aladdin biochemical Technology Co., Ltd (Shanghai, China). Sodium azide (NaN_3) was obtained from Fuchen Chemical Reagents Company (Tianjin, China). The DNA oligonucleotides (left to right: 5′ to 3′) were synthesized and purified by Shanghai Sangon Biotech. Co. Ltd (Shanghai, China). The sequence is shown below:

Thrombin-binding aptamer
AGTCCGTGGTAGGGCAGGTTGGGGTGACT
Alkynyl modified cDNA
AGTCACCCCAACCTGCCCTACCACGGACT-≡

All other chemicals were analytical grade and used directly without further purification. Aqueous solutions were prepared with Milli-Q system (18.2 MΩ cm). Unless otherwise pointed out, all studies were carried out at room temperature.

2.2. Instruments

The surface area, pore size, and pore volume were determined by N_2 adsorption-desorption isotherms obtained at 77 K on a Micromeritics ASAP 2020. The transmission electron microscopy (TEM) images were obtained with TecnaiG2 F20 S-TWINTEM (FEI, USA). Fourier transform infrared spectroscopy (FT-IR) was performed on a Nicolet 6700 (Thermo Fisher Scientific, USA) spectrometer by transmission mode. Fluorescence measurements were carried out on a 970-CRT fluorescence spectrometer (Hitachi Ltd., Shanghai, China) using a square quartz cuvette (200 μL). Excitation and emission slits were all set for a 10.0 nm band-pass. The excitation wavelength was set at 495 nm, and the emission spectra were collected from 520 to 600 nm. The fluorescence intensity at 525 nm was used to evaluate the performances of the proposed assay strategy. All nanoparticles were centrifuged on a TG16-W centrifuge (Hunan, China).

2.3. Preparation of N_3-MSN

MSN was synthesized according to the literatures [31,32]. Briefly, 0.5 g of CTAB was initially dissolved in 240 mL distilled water, and then 1.75 mL sodium hydroxide (2.0 M) was slowly added to the CTAB solution with vigorous stirring for 30 min at 333 K to get a clear and transparent solution. Afterwards, TEOS (2.5 mL) was dropped to the above prepared solution slowly, followed by vigorously stirring for 2 h until white precipitates were obtained. The product was filtered, washed with distilled water and methanol in order, and then dried in air. The mixture of synthesized MSN (700 mg) and TMCS (700 μL) was refluxed 20 h in the presence of anhydrous toluene (60 mL) to obtained the modified MSN with the template of chlorosilane (MSN-Cl-CTAB). To remove the CTAB, MSN-Cl-CTAB (500 mg) was dispersed in 50 mL of methanol containing HCl (0.50 mL, 37.2%) and the mixed solution was refluxed for another 24 h. Then the solid was washed with double-distilled water and anhydrous ethanol after centrifugation. To remove the solvent in the pore, the material without template was dried at 333 K and it was denoted as MSN-Cl. To finally produce N_3-MSN, MSN-Cl (100 mg) was dispersed in anhydrous DMF (40 mL), followed by slowly adding NaN_3 (100 mg) with stirring for 5 h at ice water.

2.4. Preparation of FITC-loading N_3-MSN capped with double stranded DNA

The loading of FITC into the pores of N_3-MSN was prepared according to the literature [33,34]. Thrombin aptamer (50 μM) was hybridized with complementary DNA (cDNA, 40 μM) to produce a dsDNA in phosphate-buffered saline (PBS, pH 7.4) for 1 h at 310 K. To ensure cDNA entirely hybridize with aptamer, the concentration of aptamer was higher than that of cDNA. N_3-MSN (4 mg) was initially dispersed into PBS (2 mL, pH 6.8) containing FITC (2 mg), and the resulting mixture was then gently shaken in the thermomixer for 16 h at room temperature. During this process, FITC was diffused into the pores of the N_3-MSN. Then dsDNA (60 μL), CuI (1 μL) and TBTA (2 μL) were added to the suspension. The mixture was gently stirred for 4 h at 310 K. Alkynyl modified dsDNA can be modified on the surface of N_3-MSN through the click chemistry reaction with high efficiency. Finally, the dsDNA capped N_3-MSN loaded with FITC (designated as dsDNA-FITC-MSN) was dispersed into PBS buffer and kept at 277 K for further using.

2.5. Detection of thrombin

dsDNA-FITC-MSN (10 mL) and different concentrations of thrombin were added to PBS buffer (180 μL), then the solution was gently shaken on the thermomixer for 40 min at room temperature. Then the mixture was centrifuged and the fluorescence of supernatant was detected (λ_{ex} = 490 nm, λ_{em} = 520 nm).

3. Results and discussion

3.1. The principle of biosensor for thrombin detection based on stimulus-response controlled release system

Scheme 1 shows the principle of the fluorescence biosensor for thrombin detection based on stimulus-response controlled release system. The biosensor consists of three parts: the controlled release material, the target recognition, and the signal transduction parts. Alkynyl modified cDNA was hybridized with the aptamer of thrombin to form dsDNA firstly and then reacted with the N_3-MSN through CuAAC,

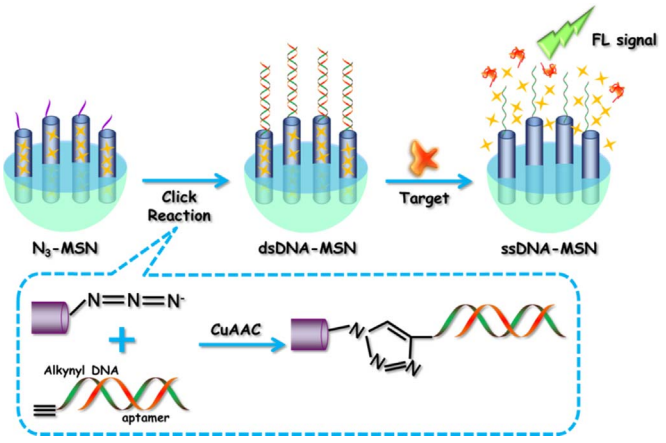

Scheme 1. Schematic illustration of aptamer-functionalized mesoporous silica nanoparticles based controlled release system for thrombin detection.

the combined dsDNA could block FITC in the pores of the MSN with high efficiency. After the addition of the target (thrombin), thrombin-aptamer complex rather than aptamer-cDNA duplex was formed, the dsDNA on the surface of MSN was decomposed into ssDNA. Because only cDNA cannot cap the pores of MSN efficiency, the FITC was released into the solution and enhanced fluorescence signal was detected. The enhanced fluorescence had a relationship with the amount of thrombin. On the basis of this principle, a sensitive fluorescence biosensor can be developed for thrombin detection.

Simple assay was carried out to verify the proposed principle. As shown in Fig. 1, low background signal was detected in the blank solution (dsDNA-FITC-MSN in PBS solution, line a) after four-week storage, suggesting the pores of MSN are blocked by the dsDNA with high efficiency and nearly no leakage of FITC occurs. On the contrary, a strong fluorescence signal was detected when different levels of thrombin were added to the above-mentioned system (line b and c). This phenomenon indicates that FITC is released from the pores of MSN and higher concentration of thrombin can result in stronger fluorescence intensity. If MSN loaded with FITC was not gated by the dsDNA, a strong fluorescence signal enhancement was detected without the addition of target (line d), this is probably because the FITC can be easily diffused into the solution. These phenomena demonstrate the feasibility of the proposed biosensor.

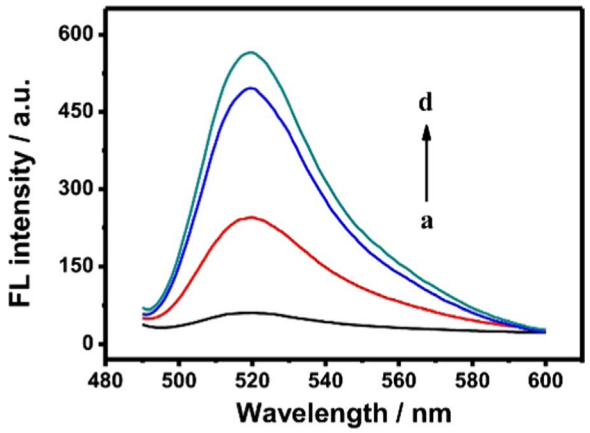

Fig. 1. Fluorescence spectra under different conditions: (a) dsDNA-FITC-MSN in PBS solution; (b) dsDNA-FITC-MSN treated with 125 ng mL^{-1} thrombin solution; (c) dsDNA-FITC-MSN treated with 1000 ng mL^{-1} thrombin solution; (d) MSN loaded with FITC and unblocked with the dsDNA dispersed in PBS solution.

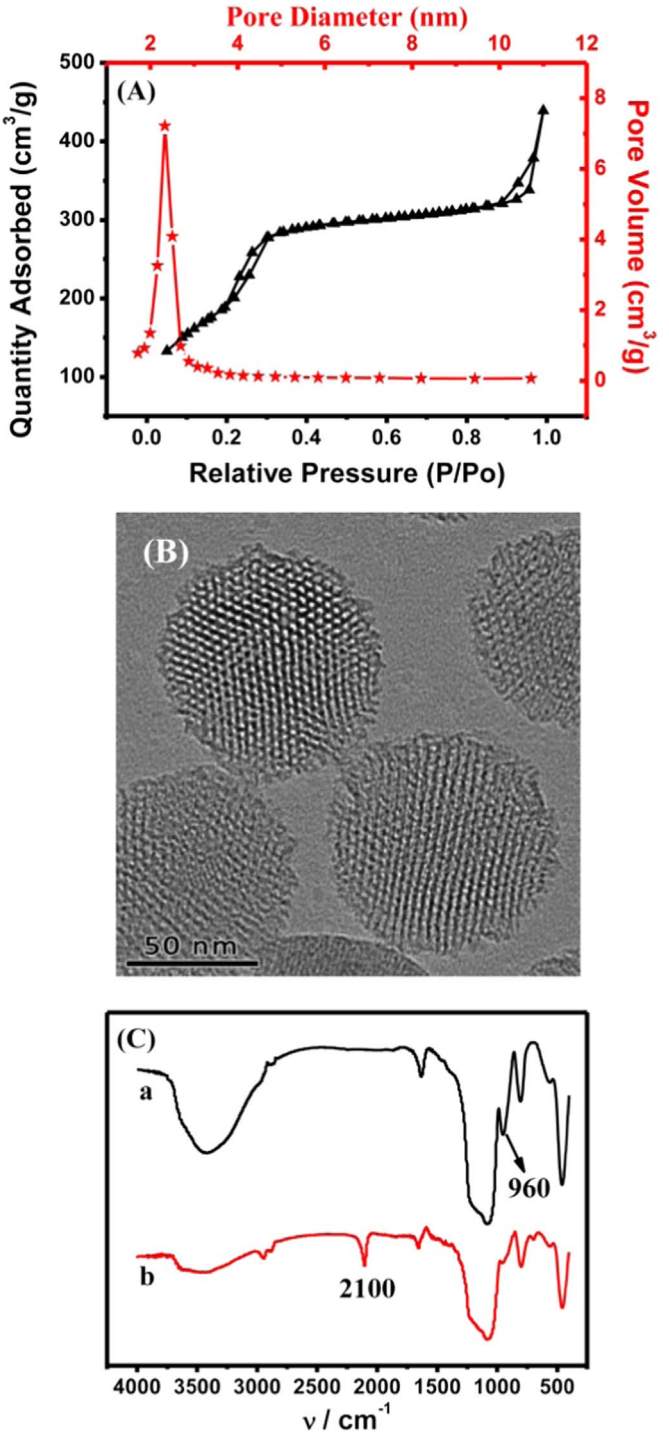

Fig. 2. (A) Nitrogen sorption isotherms of the as-prepared N_3-MSN measured at 77.156 K. and the BJH pore distribution curve based on the adsorption isotherm; (B) TEM image of N_3-MSN; (C) FTIR spectra of (a) MSN and (b) N_3-MSN.

3.2. Characterization of the as-synthesized MSN

Fig. 2A shows the N_2 adsorption-desorption isotherms and pore size distribution of the N_3-MSN. The mesopore diameter was measured to be 2.3 nm by the Barrett-Joyner-Halenda (BJH) method while the specific surface area and pore volume were measured to be 756 $m^2 g^{-1}$ and 0.32 $cm^3 g^{-1}$ by the Brunauer–Emmett–Teller (BET) method, these results obey the typical features of mesoporous materials. TEM image in Fig. 2B shows a typical image of the prepared N_3-MSN, the average size of the as-synthesized MSN was 85 nm. This result indicates the N_3-MSN

possesses excellent mesoporous channels structure. Meanwhile, a large number of pores on the silica nanospheres were observed and the pore size was 3 nm in average [35–37]. Furthermore, the surface functionalization was confirmed by FTIR. Fig. 2C shows FTIR spectra for MSN and N_3-MSN nanoparticles. Apparently, after MSN were modified with azide groups (line b), vibration peaks which can be assigned to the stretching bands of azide groups were observed at 2100 cm^{-1}; the Si-OH band at 960 cm^{-1} became significantly weaker [38–40]. These results indicate that azide groups are successfully modified onto MSN.

3.3. Optimization of the experimental conditions

Some key experimental conditions such as the amount of dsDNA used to cap the pores of N_3-MSN, the pH of the controlled release system, and the incubation time between thrombin-aptamer reactions were optimized to acquire the best performance of the proposed biosensor. A small amount of dsDNA cannot block the pores of MSNs effectively, and FITC may leak into the system, so strong background signal can be detected. Whereas excess amount of dsDNA can cap the pores of MSNs effectively and hence reduces the leakage of FITC, but more targets are needed to open the gate, which results in the lower sensitivity of the proposed biosensor. So the concentration of dsDNA used to cap on the N_3-MSN surface was optimized firstly. As shown in Fig. 3A, the background signal of the system reduced with the increase of dsDNA concentration firstly and then reached a plateau at 25 nM. This result indicates that 25 nM is enough to block the pores, so 25 nM was chosen as the optimum concentration. The pH of the buffer can affect the activity of the thrombin. Thus, the pH of the controlled release system interaction solution was also optimized. As shown in Fig. 3B, the thrombin lost its activity at low and high pH values, so little fluorescence enhancement was observed after the addition of the target. Therefore, pH 7.2 was used in this controlled release system. The reaction time between dsDNA and thrombin also affects the fluorescence enhancement of the proposed system. As shown in Fig. 3C, the fluorescence intensity of the system seldom changed without addition of thrombin, suggesting little leakage of FITC from the pores of MSN occurs. But the fluorescence intensity of the system increased with the reaction time and reached a plateau after 60 min. So 60 min was chosen as the optimized condition in the following study.

3.4. Calibration curve for thrombin detection

Different concentrations of thrombin were added to examine the fluorescence response of the proposed system. Fig. 4A shows that the fluorescence intensity of the system increased with the increase of thrombin concentration. The fluorescence intensity had a linear relationship with the logarithm of the thrombin concentration in the range of 50–1000 ng mL^{-1} (shown in Fig. 4 B) with the following regression equation was

$$I = 273.5 \log C - 366.8$$

where I represents the fluorescence intensity and C is the concentration of thrombin. The regression coefficient was 0.9939 and the limit of detection (LOD) was calculated to be 28.46 ng mL^{-1} (S/N = 3). Compared with other reported methods for thrombin detection, such as enzyme-linked immunosorbent assay (ELISA), colorimetric, fluorescence, etc. (summarized in Table 1), through the LOD is not the best, it is at the same level with the other reported fluorescence method [41] and no amplification procedures is need. Furthermore, the presented study is to offer a new strategy to construct a control release system with higher stability, in which the pores of mesoporous silica nanoparticles were capped by aptamer through click chemistry reaction for the first time. Compared with the capping strategy using aptamer via electrostatic interaction, the capping strategy using aptamer via click chemistry has high efficiency and nearly no leakage exists, so the stability is good. If dsDNA-FITC-MSN was stored in a refrigerator (4 °C, 3 weeks) and then used to detect the target, the result is nearly the same as that of the fresh prepared one, this outcome directly indicates that the prepared material has good stability. Seven parallel experiments were performed (thrombin concentration: 100 ng mL^{-1}), the relative standard deviation (RSD) was calculated to be 2.7%. This result indicates that the proposed method has good reproducibility.

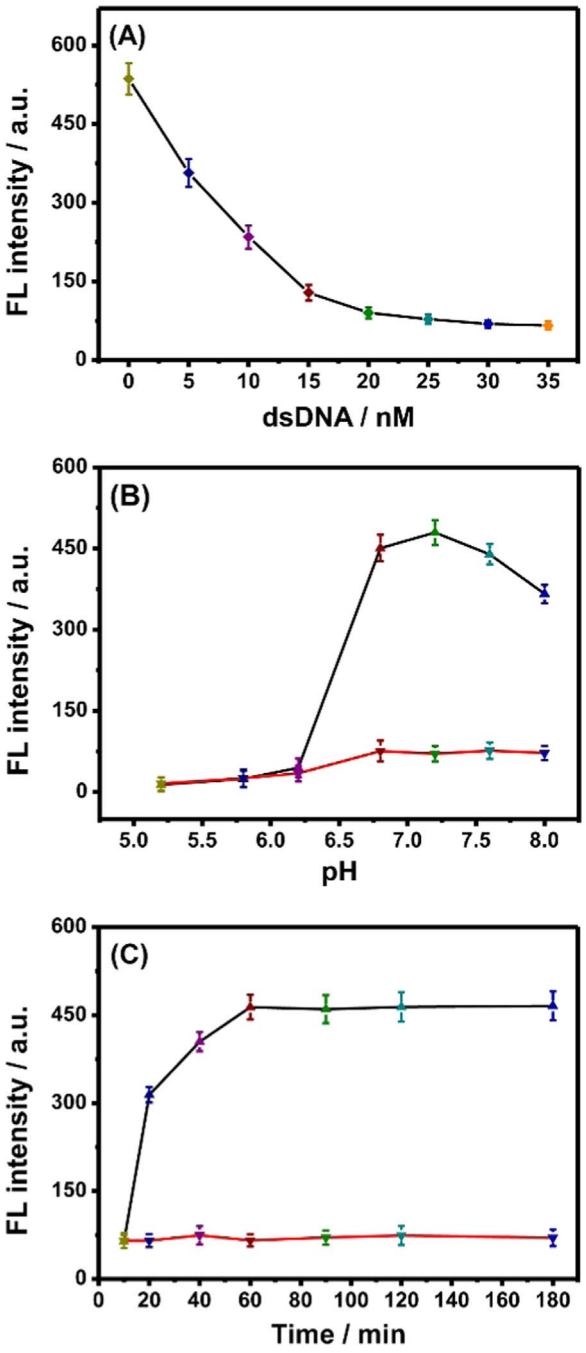

Fig. 3. Conditions optimization for the control release system: (A) Variance of fluorescence intensity with the dsDNA concentration; (B) Variance of fluorescence intensity in the presence of absence of the thrombin with different pH in control release system. (C) Variance of the fluorescence intensity in the presence of absence of the thrombin in control release system.

3.5. Selectivity and application of the proposed biosensor

To evaluate the selectivity of the developed biosensor, several proteins such as human serum protein (HSA), lysozyme (lys), glucose

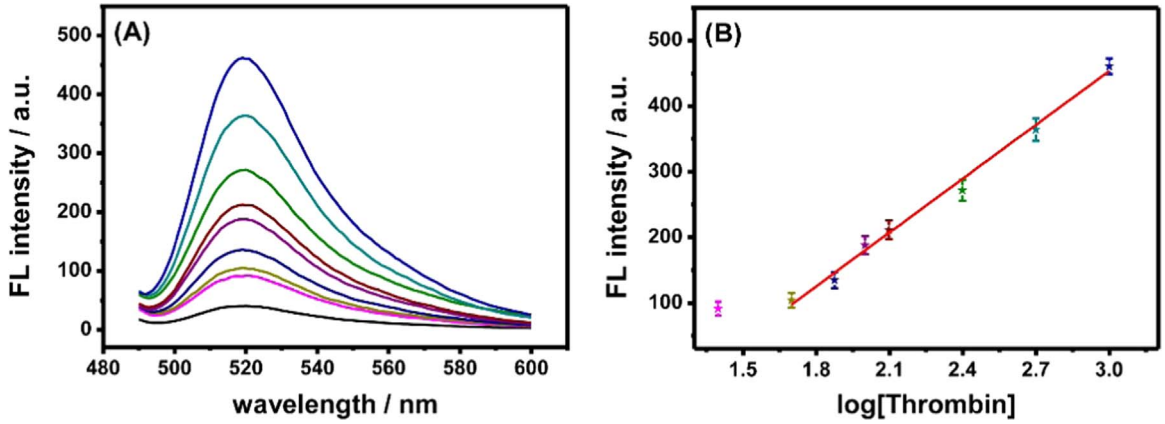

Fig. 4. (A) Fluorescence intensity of the system at different thrombin concentrations. From bottom to top: 50, 75, 100, 125, 250, 500, 1000 ng mL^{-1}; (B) Calibration curve between the fluorescence intensity and the thrombin concentrations.

Table 1
Comparison of the different methods for thrombin detection.

	Method	LOD	Reference
1	Fluorescence	8.4 nM	[41]
2	Surface-Enhanced Raman Scattering	1 pM	[42]
3	Paper Electrochemical Device	16 nM	[43]
4	Electrochemistry	5.7 fM	[44]
5	Colorimetric	0.04 pM	[45]
6	Electrochemiluminescence	0.12 pM	[46]
7	Fluorescence	8.131 nM	This work*

* In this work, the LOD was 28.46 ng mL^{-1}, which is about 8.131 nM ($M_{thrombin}$ = 35 KD).

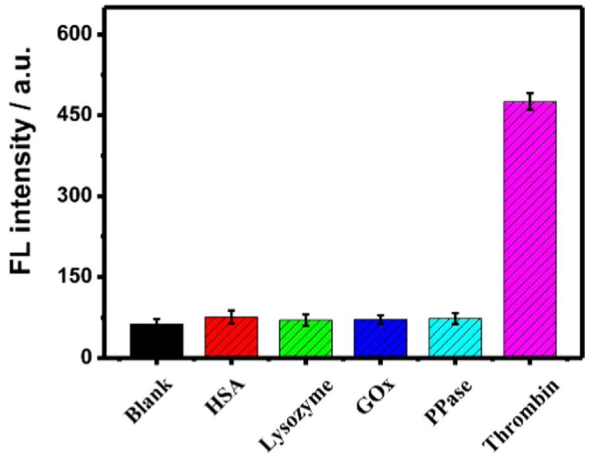

Fig. 5. Selectivity of the proposed fluorescence biosensor for thrombin detection (the concentrations of analytes were 1000 ng mL^{-1} and others were 10 μg mL^{-1}).

oxidase (GOx) and pyrophosphatase (PPase) were chosen as the potential interferents. The concentration of interferents was settled as 10 μg mL^{-1} and that of thrombin was 1 μg mL^{-1}. As shown in Fig. 5, the presence of interferents has little influence on the fluorescence intensity of the system, but significant fluorescence enhancement was observed in the presence of thrombin with relatively lower concentration. The reason lies in that these interferents are unable to combine with the aptamer and hence cannot destroy the complexation between MSN and aptamer, so no FITC is diffused into the solution and no fluorescence enhancement appears. These results indicate that the proposed method owns high selectivity.

The proposed system was then applied to detect thrombin in human serum (provided by the volunteers from the First Affiliated Hospital of Fujian Medical University (Fujian, China)). As no coagulation factors were contained in healthy human serum sample, thrombin is in the form of prothrombin in the serum samples [46,47]. Thus, standard addition experiments were performed with the serum samples to validate the determination. The obtained results were compared with those using conventional ELISA method (summarized in Table 2). Apparently, the values detected by the proposed method have good accordance with those by the ELISA method. Good recovery rate and precision suggest that our method is reliable.

4. Conclusions

In summary, a highly selective and sensitive fluorescent biosensor has been successfully developed for thrombin detection, in which click chemistry was firstly applied in controlled release system. The capping process via click chemistry reaction enables the nearly zero leakage, so such proposed biosensor has good stability, high selectivity and reproducibility and it has been successfully applied to detect thrombin in human serum samples with satisfied results. Furthermore, the proposed biosensor offers a new strategy for sensitive detection of targets which have aptamers via the controlled release system.

Table 2
Recovery of thrombin in human serum samples obtained by the proposed method and a commercial ELISA method (n = 3).

Sample number	Added concentration (ng mL^{-1})	Method (mean SD, ng mL^{-1}) and recovery rate (%)		Relative error of the results (%)
		Our method	ELISA	
1	75.00	70.15 ± 5.37 (93.53)	77.61 ± 2.05 (103.5)	− 9.612
2	125.0	119.8 ± 3.27 (95.84)	123.6 ± 1.89 (98.88)	− 3.074
3	200.0	192.3 ± 2.05 (96.15)	198.2 ± 1.69 (99.10)	− 2.977
4	400.0	414.6 ± 1.61 (103.7)	409.2 ± 1.72 (102.3)	1.320
5	800.0	832.3 ± 3.11 (104.0)	Overflow	–

Acknowledgements

This work was financially supported by the National Science Foundation of China (21575025, 21575027 and 21575028), the Program for Changjiang Scholars and Innovative Research Team in University (No. IRT15R11), and the Foundation for Scholars of Fuzhou University (No. XRC-1671).

References

[1] Z. Li, J.C. Barnes, A. Bosoy, J.F. Stoddart, J.I. Zink, Chem. Soc. Rev. 41 (2012) 2590–2605.
[2] Q. He, J. Shi, J. Mater. Chem. 21 (2011) 5845–5855.
[3] B.G. Trewyn, I.I. Slowing, S. Giri, H.-T. Chen, V.S.-Y. Lin, Acc. Chem. Res. 40 (2007) 846–853.
[4] Y. Zhao, B.G. Trewyn, I.I. Slowing, V.S.-Y. Lin, J. Am. Chem. Soc. 131 (2009) 8398–8400.
[5] I.I. Slowing, J.L. Vivero-Escoto, C.-W. Wu, V.S.-Y. Lin, Adv. Drug Deliv. Rev. 60 (2008) 1278–1288.
[6] J.L. Vivero-Escoto, I.I. Slowing, B.G. Trewyn, V.S.Y. Lin, Small 6 (2010) 1952–1967.
[7] C.-L. Zhu, C.-H. Lu, X.-Y. Song, H.-H. Yang, X.-R. Wang, J. Am. Chem. Soc. 133 (2011) 1278–1281.
[8] R. Liu, X. Zhao, T. Wu, P. Feng, J. Am. Chem. Soc. 130 (2008) 14418–14419.
[9] T.D. Nguyen, Y. Liu, S. Saha, K.C.-F. Leung, J.F. Stoddart, J.I. Zink, J. Am. Chem. Soc. 129 (2007) 626–634.
[10] N.K. Mal, M. Fujiwara, Y. Tanaka, Nature 421 (2003) 350–353.
[11] A. Schlossbauer, J. Kecht, T. Bein, Angew. Chem. Int. Ed. 121 (2009) 3138–3141.
[12] C. Park, K. Oh, S.C. Lee, C. Kim, Angew. Chem. Int. Ed. 46 (2007) 1455–1457.
[13] E. Aznar, L. Mondragón, J.V. Ros-Lis, F. Sancenón, M.D. Marcos, R. Martínez-Máñez, J. Soto, E. Pérez-Payá, P. Amorós, Angew. Chem. Int. Ed. 123 (2011) 11368–11371.
[14] N.Ž. Knežević, B.G. Trewyn, V.S.-Y. Lin, Chem. Comm. 47 (2011) 2817–2819.
[15] K. Patel, S. Angelos, W.R. Dichtel, A. Coskun, Y.-W. Yang, J.I. Zink, J.F. Stoddart, J. Am. Chem. Soc. 130 (2008) 2382–2383.
[16] E. Climent, A. Bernardos, R. Martinez-Manez, A. Maquieira, M.D. Marcos, N. Pastor-Navarro, R. Puchades, F. Sancenón, J. Soto, P. Amorós, J. Am. Chem. Soc. 131 (2009) 14075–14080.
[17] E. Climent, R. Martínez-Máñez, F. Sancenón, M.D. Marcos, J. Soto, A. Maquieira, P. Amorós, Angew. Chem. Int. Ed. 122 (2010) 7439–7441.
[18] L.L. Li, Q. Yin, J. Cheng, Y. Lu, Adv. Healthc. Mater. 1 (2012) 567–572.
[19] L. Hou, C. Zhu, X. Wu, G. Chen, D. Tang, Chem. Comm. 50 (2014) 1441 – 1143.
[20] Y. Zhang, Q. Yuan, T. Chen, X. Zhang, Y. Chen, W. Tan, Anal. Chem. 84 (2012) 1956–1962.
[21] Z. Chen, Y. Tan, K. Xu, L. Zhang, B. Qiu, L. Guo, Z. Lin, G. Chen, Biosens. Bioelectron. 75 (2016) 8–14.
[22] H.C. Kolb, M. Finn, K.B. Sharpless, Angew. Chem. Int. Ed. 40 (2001) 2004–2021.
[23] J.E. Moses, A.D. Moorhouse, Chem. Soc. Rev. 36 (2007) 1249–1262.
[24] W.H. Binder, R. Sachsenhofer, Macromol. Rapid Commun. 28 (2007) 15–54.
[25] C.R. Becer, R. Hoogenboom, U.S. Schubert, Angew. Chem. Int. Ed. 48 (2009) 4900–4908.
[26] S. Qiu, S. Gao, Q. Liu, Z. Lin, B. Qiu, G. Chen, Biosens. Bioelectron. 26 (2011) 4326–4330.
[27] Y. Hori, H. Ueno, S. Mizukami, K. Kikuchi, J. Am. Chem. Soc. 131 (2009) 16610–16611.
[28] Y. Yao, D. Tian, H. Li, ACS Appl. Mater. Interfaces 2 (2010) 684–690.
[29] N.M. Moore, N.J. Lin, N.D. Gallant, M.L. Becker, Biomaterials 31 (2010) 1604–1611.
[30] J. Huntington, J. Thromb. Haemost. 3 (2005) 1861–1872.
[31] M. Vallet-Regi, A. Rámila, R.P. del Real, J. Pérez-Pariente, Chem. Mater. 13 (2001) 308–311.
[32] C. Chen, J. Geng, F. Pu, X. Yang, J. Ren, X. Qu, Angew. Chem. Int. Ed. 50 (2011) 882–886.
[33] B. Malvi, B.R. Sarkar, D. Pati, R. Mathew, T.G. Ajithkumar, S. Sen Gupta, J. Mater. Chem. 19 (2009) 1409–1416.
[34] D.G. He, X.X. He, K.M. Wang, M.A. Chen, Y.X. Zhao, Z. Zou, J. Mater. Chem. B 1 (2013) 1552–1560.
[35] N. Sun, J. Wang, J. Yao, C. Deng, Anal. Chem. 89 (2017) 1764–1771.
[36] Y. Chen, D. Li, Z. Bie, X. He, Z. Liu, Anal. Chem. 88 (2016) 1447–1454.
[37] Z. Qiu, J. Shu, D. Tang, Anal. Chem. 89 (2017) 5152–5160.
[38] Y. Goto, H. Sato, S. Shinkai, K. Sada, J. Am. Chem. Soc. 130 (2008) 14354–14355.
[39] J. Bang, J. Bae, P. Lowenhielm, C. Spiessberger, S.A. Given-Beck, T.P. Russell, C.J. Hawker, Adv. Mater. 19 (2007) 4552–4557.
[40] D. Quemener, T.P. Davis, C. Barner-Kowollik, M.H. Stenzel, Chem. Commun. (2006) 5051–5053.
[41] Y. Zhu, X. Hu, S. Shi, R. Gao, H. Huang, Y. Zhu, X. Lv, T. Yao, Biosens. Bioelectron. 79 (2016) 205–212.
[42] X. Chen, H. Liu, X. Zhou, J. Hu, Nanoscale 2 (2010) 2841–2846.
[43] J. Cunningham, N. Brenes, R. Crooks, Anal. Chem. 86 (2014) 6166–6170.
[44] L. Xu, S. Wang, H. Dong, G. Liu, Y. Wen, S. Wang, X. Zhang, Nanoscale 4 (2012) 3786–3790.
[45] C. Chen, C. Huang, H. Chang, Biosens. Bioelectron. 25 (2010) 1922–1927.
[46] G. Jie, J. Yuan, Anal. Chem. 84 (2012) 2811–2817.
[47] S. Xie, J. Ye, Y. Yuan, Y. Chai, R. Yuan, Nanoscale 7 (2015) 18232–18238.